Identification Card and Codification of the Chemical and Morphological Characteristics of 14 Dental Implant Surfaces

David M. Dohan Ehrenfest, DDS, MS, PhD[1]*
Lydia Vazquez, MD, DDS[2]
Yeong-Joon Park, DDS, PhD[3]
Gilberto Sammartino, MD, DDS[4]
Jean-Pierre Bernard, MD, PhD[2]

Dental implants are commonly used in daily practice; however, most surgeons do not really know the characteristics of these biomedical devices they are placing in their patients. The objective of this work is to describe the chemical and morphological characteristics of 14 implant surfaces available on the market and to establish a simple and clear identification (ID) card for all of them, following the classification procedure developed in the Dohan Ehrenfest et al (2010) Codification (DEC) system. Fourteen implant surfaces were characterized: TiUnite (Nobel Biocare), Ospol (Ospol), Kohno HRPS (Sweden & Martina), Osseospeed (AstraTech), Ankylos (Dentsply Friadent), MTX (Zimmer), Promote (Camlog), BTI Interna (Biotechnology Institute), EVL Plus (SERF), Twinkon Ref (Tekka), Ossean (Intra-Lock), NanoTite (Biomet 3I), SLActive (ITI Straumann), Integra-CP/NanoTite (Bicon). Three samples of each implant were analyzed. Superficial chemical composition was analyzed using X-ray photoelectron spectroscopy/electron spectroscopy for chemical analysis, and the 100 nm in-depth profile was established using Auger electron spectroscopy. The microtopography was quantified using light interferometry. The general morphology and nanotopography were evaluated using a field emission-scanning electron microscope. Finally, the characterization code of each surface was established using the DEC system, and the main characteristics of each surface were summarized in a reader-friendly ID card. From a chemical standpoint, of the 14 different surfaces, 10 were based on a commercially pure titanium (grade 2 or 4), 3 on a titanium-aluminum alloy (grade 5 titanium), and one on a calcium phosphate core. Nine surfaces presented different forms of chemical impregnation or discontinuous coating of the titanium core, and 3 surfaces were covered with residual aluminablasting particles. Twelve surfaces presented different degrees of inorganic pollutions, and 2 presented a severe organic pollution overcoat. Only 2 surfaces presented no pollution (Osseospeed and Ossean). From a morphological standpoint, 2 surfaces were microporous (anodization) and 12 were microrough, with different microtopographical aspects and values.

[1] LoB5 unit, Chonnam National University School of Dentistry, Gwangju, South Korea.
[2] Department of Stomatology, Oral Surgery and Dento-maxillofacial Radiology, School of Dental Medicine, University of Geneva, Geneva, Switzerland.
[3] Department of Biomaterials, Chonnam National University School of Dentistry, Gwangju, South Korea.
[4] Department of Oral Surgery, University Federico II, Naples, Italy.
**Corresponding author*, e-mail: LoB5@mac.com
DOI: 10.1563/AAID-JOI-D-11-00080

Ten surfaces were smooth on the nanoscale, and therefore presented no significant and repetitive nanostructures. Four implants were nanomodified: 2 implants were nanorough (Osseospeed and Ossean), and 2 were covered with nanoparticles (NanoTite and SLActive). TiUnite and Kohno HRPS were covered with extended cracks all over the surface. Only 8 surfaces could be considered homogeneous. This systematic approach allowed the main characteristics of these commercially available products to be gathered in a single ID card. It can be used as an experimental tool or a method for controlling industrial implant productions. The DEC system could be an interesting basis for the development of a clear and simple ISO standard for dental implant surfaces and other implantable devices.

Key Words: dental implant, nanostructure, osseointegration, titanium

Dental implants are now commonly used in daily practice, but most surgeons have very limited information concerning the characteristics of the products they use.[1] These implants interact with living tissues and functions and therefore have at least 2 main characteristics that should be clearly available to customers: biomechanical characteristics of the macrodesign and chemical/physical characteristics of the osseointegrated interface.[2] In fact, many parameters influence the process of osseointegration and the protection of the peri-implant bone tissue, particularly the surface modifications[3–10] and the macrodesign of the implant,[3,11–18] but also the general physiological conditions of the patients,[19–23] the bone quality and quantity of the implantable sites,[24–25] the surgical procedure,[26–29] and the prosthetic functional loading procedure[30] and timing.[31–33] All these parameters are the source of a large literature and scientific debates. However the surface characteristics are intrinsic industrial parameters of the product and should therefore be clearly disclosed to the users.

Even if most companies advertise some surface characteristics of their products, no clear certified data are easily available for the surgeon.[1] The main reason for this difficulty in obtaining information about the surface characteristics is that the scientific literature on dental implant surfaces is quite confusing, and no global standard has yet been developed or is widespread. However, the analysis of surfaces is a well-known science that is used in various fields such as the semiconductor and chemical industries. Therefore, numerous instruments can be used to characterize dental implant surfaces, and some articles have already started to accurately describe the chemical composition,[34,35] microtopography,[36] and nanotopography of some commercially available products.[37–39] However, accurate data remain scarce and are difficult to interpret and standardize.

Recently, a classification system was published to create a standard for characterizing dental implant surfaces.[2] Using standardized tools of analysis and terminology, each osseointegrated implant surface can be defined using a characterization code. The characterization code first describes the surface chemical composition: the core material (titanium grade, zirconia, hydroxyapatite) and the chemical or biochemical modification (impregnation, coating, pollution). The code then defines the surface morphological characteristics (topography, structures) at the micrometer (microroughness, micropores) and nanometer (nanosmooth, nanoroughness, nanopatterning, nanotubes, nanoparticles) scales. Finally, the characterization code is completed with information about the general morphology of the implant surface, such as its homogeneity, the presence of cracks or large particle inclusions, and the possibility of a fractal dimension between the 3 levels of investigation (microscale, nanoscale, and atomic scale). This standardized codification system allows users to clarify the identity of each surface and to easily sort their differences. However, it is still necessary to gather the analytical data in a simple way in order to present the data in a reader-friendly way for the users of these products.

The objective of this article is to describe the chemical and morphological characteristics of 14 implant surfaces available on the market and to establish a simple and clear identification (ID) card for all of them, following the classification procedure developed in the Dohan Ehrenfest et al (2010) Codification (DEC) system.[2]

Materials and Methods

Fourteen implant surfaces were investigated: TiUnite (Nobel Biocare, Gothenburg, Sweden), Ospol (Ospol, Höllviken, Sweden), Kohno HRPS (Sweden & Martina, Due Carrare, Italy), Osseospeed (AstraTech, Mölndal, Sweden), Ankylos (Dentsply Friadent, Mannheim, Germany), MTX (Zimmer, Carlsbad, Calif), Promote (Camlog, Basel, Switzerland), BTI Interna (Biotechnology Institute, Vitoria, Spain), EVL Plus (SERF, Decines, France), Twinkon Ref (Tekka, Brignais, France), Ossean (Intra-Lock, Boca Raton, Fla), NanoTite (Biomet 3I, Palm Beach Gardens, Fla), SLActive (ITI Straumann, Basel, Switzerland), and Integra-CP/NanoTite (Bicon, Boston, Mass). Three samples were used per implant system, and their reference and batch are reported in their respective ID card.

Chemical analyses

The chemical characteristics of the surfaces were evaluated using 2 investigative techniques.

The superficial atomic composition and chemistry of all the samples were evaluated accurately through X-ray photoelectron spectroscopy (XPS)/electron spectroscopy for chemical analysis (ESCA) using a PHI Quantum 2000 instrument (Physical Electronics Inc, Chanhassen, Minn; analytical parameters: monochromatic X-ray source Alkα 1486.6eV, acceptance angle $\pm 23^\circ$, take-off angle 45°, charge correction C1s 284.8 eV) on a 100 μm diameter analysis area located between the second and third threads of each sample. This technique allows the surface chemistry of a 5–10 nm thick superficial layer to be analyzed.

The in-depth analysis of the chemical composition of the external surface layer was performed using Auger electron spectroscopy (AES) using a PHI 670 Scanning Auger Nanoprobe instrument (Physical Electronics Inc; Electron Beam Energy 10keV, 20nA; Tilt 30° to sample normal) on a very small analysis area (30 nm in diameter) located in the middle of the cutting edge (or an equivalent flat part, depending on the implant macrodesign) of each implant. The in-depth chemical profile was established down to 100 nm, using sputtering cycles with a 4keV Ar+ source (Ar+ etching rate for TiO_2: 3.3 nm/min). Two in-depth profiles were established per sample. The analysis area being very small, the 2 spots were very precisely located, respectively, on a peak and in a valley of the surface microtopography.

Morphological analysis

The morphological characteristics of the surfaces were evaluated using 2 techniques of investigation.

The general morphology of the surfaces was evaluated and described separately by 2 independent teams, the first one with a field emission-scanning electron microscope (FE-SEM, Hitachi S-4700, Hitachi

TABLE
Complete codification system for the microtopography of osseointegrated implant surfaces

	1/ Morphology Type (No. of dimensions [D])
R	Rough (1D)
Pa/Po	Patterned or Porous (2D)
X-Pt	Particle (3D): X = elemental composition
	2/ Height Deviation Amplitude (Sa)
S	Smooth: Sa = 0 to 0.5 μm
Mi	Minimal: Sa = 0.5 to 1 μm
Mo	Moderate: Sa = 1 to 2 μm
Ma	Maximal: Sa > 2 μm
	3/ Spatial Density (developed area ratio, Sdr%)
Fl	Flat: Sdr% = 0 to 50%
Fo	Flattened out: Sdr% = 50 to 100%
Ru	Rugged: Sdr% = 100 to 200%
eRu	Extra rugged: Sdr% > 200%

HTA, Pleasanton, Calif) up to ×200 000 magnification and the second one with a classical scanning electron microscope (SEM; LV-6380, JEOL, Tokyo, Japan). All the areas of the implants were carefully examined, from the macroscale to the nanoscale. This examination allowed the various morphological characteristics of the surfaces (cracks, blasting residues, homogeneity) to be highlighted and allowed for determination of the kind of nanotopography of each sample (nanosmooth, nanorough, nanopatterned, or nanoparticled).

The microtopography was quantified using a light interferometer (IFM, MicroXAM, ADE Phase Shift Inc, Tucson, Ariz), following the guidelines suggested in 2000,[36] that is, evaluating the topography on the top, valley, and flank of 3 successive threads and calculating the corrected mean values of these large areas. The dimensions of the analyzed areas were 200 × 260 μm most of the time, but the area could be a little bit smaller depending on the implant macrogeometry. An IFM three-dimensional reconstruction picture was used in each ID card to illustrate the general aspect of the microtopography. Several topographical parameters were assessed, but only 2 were considered significant for the classification of the surface characteristics: the Sa (height deviation amplitude of the microtopography, also called roughness) and the Sdr% (a hybrid parameter integrating both the number and height of peaks of the microtopography). The Sa is an important and frequent parameter for comparing surfaces and has already been used in other classifications.[40] The Sdr% is calculated as a developed area ratio relative to a flat plane baseline. For a totally flat surface, Sdr = 0%. When Sdr = 100%, it means that the roughness of a surface doubled its developed area.

These Sa and Sdr% values allowed for classification of the microtopography, following the previously developed DEC system. However, we have introduced some minor modifications to the initial classification system: when Sdr% is below 50%, the surface is labeled ''flat'', and when the Sdr% is above 200%, the surface is labeled ''extra rugged''. The modified classification system for these values is summarized in the Table.

RESULTS

General considerations

XPS is a very sensitive technique that allows the user to determine the relative quantities and chemical states of most elements present on the surface, main elements and various contaminants. The high-resolution spectra of these analyses allows determination of the atomic links, and therefore clarifies the surface chemistry. For example, all the surfaces present significant percentages of carbon, and the XPS clarifies whether the carbon is related to adventitious carbon from the atmosphere or organic contaminants. The oxygen is associated with titanium oxides, carbon contaminants, and adsorbed water on the superficial layer. It can also be detected as Al_2O_3 when alumina-blasting residues are present on a surface. For the establishment of the ID cards, the XPS data are only provided in a simplified table of atomic composition, where significant variations are highlighted in bold type, but the high-resolution spectra were used to validate the codification of the chemistry in each card.

The AES method allows for the in-depth analysis of very small areas but with fewer details than XPS. Our protocol allowed for the analysis of the chemical composition of the first 100 nm surface thickness, which is the main interface during the osseointegration. In some surfaces, the percentage of aluminum quickly reached almost 10% of the total composition, and this is typical of grade 5 Ti-6Al-4V titanium cores. The AES profiles were often similar between the peaks and valleys, and the peak profile was used in the ID cards. Because of the very small size of the analysis spot, some elements presenting a heterogeneous distribution and detected with XPS were not found with AES. For example, alumina-blasting residues were sometimes outside the AES beam, and therefore were not detected, even if they were clearly visible with the SEM.

The combination of XPS and AES data allows the TiO_2 layer thickness to be determined, which is considered important for the osseointegration process. Typically, only anodized/oxidized implants (TiUnite and Ospol) have a very thick (micrometric) TiO_2 layer, which is considered to increase the bone/implant chemical interlocking.[41] All the other blasted and/or etched surfaces only presented a thin native TiO_2 layer (around 6–8 nm), except Ossean, which had a thicker TiO_2 layer ($>$12 nm).

The intent of these ID cards is to gather the key information about a surface in a compact format, and therefore only a limited number of FE-SEM photos can be added in each card. The FE-SEM photos are not necessary to show the microscale level of the surfaces, as the IFM three-dimensional reconstruction figures offer a much more representative and reliable illustration of the microtopography. The FE-SEM photos are thus mainly important for illustrating the global architecture of the surface and the nanoscale features. For this reason, a standard magnification of $\times$30 000 was chosen for the FE-SEM photo used in each card, because this magnification can simultaneously illustrate the microscale morphology and confirm the absence of significant nanotexture.

Sometimes, however, this standard magnification does not show the most important patterns of a surface, and another presentation is needed to keep the card reader-friendly and complete. When implant surfaces present significant and repetitive nanostructures, it is preferable to use FE-SEM photos at a higher magnification ($\times$100 000) in order to show these nanostructures very accurately. A few surfaces present large micrometric patterns that cannot be illustrated properly at the standard $\times$30 000 magnification (micropores, extended cracks). In these cases, it is more logical to use $\times$5000 photos to illustrate these surfaces clearly. Consequently, with this low magnification, the nanotopography is no longer visible, and a second photo at a higher magnification ($\times$100 000) must be provided for illustration (even if these photos look very flat when the surfaces are nanosmooth).

Note that all of these analyses have been performed and checked many times on many samples during the preliminary investigations to validate this project. Finally, we collected a last series of standardized data for the establishment of the ID cards. The surfaces were gathered in 4 groups, depending on their production technology.

Surfaces from the first group

The first group gathers all the surfaces presenting a modification of the titanium metallurgy. This includes mainly anodized or titanium plasma-sprayed (TPS) surfaces.

TiUnite (Figure 1) is an anodized surface, thus presenting a thick TiO_2 layer (>100 nm). During anodization, a high quantity of phosphorus is incorporated into the surface as a chemical modification. Inorganic fluoride and sulfate pollutions were also detected. The surface is microporous (pores created by anodization), is smooth on the nanoscale, and presents extended cracks related to the anodization process.

Ospol (Figure 2) is also an anodized surface, thus presenting a thick TiO_2 layer (>100 nm). During anodization, low quantities of calcium and phosphorus are incorporated into the surface as a chemical modification. Traces of sodium were also detected. The surface is microporous (pores created by anodization), is smooth on the nanoscale, and presents small local cracks related to the anodization process.

Kohno HRPS (High Roughness Plasma Spray) is a TPS surface (Figure 3). Some inorganic pollutions were detected: phosphorus (as phosphate), fluoride, and sulfur (as sulfate). The main characteristics of this kind of surfaces are topographical: the microroughness is maximal, it is smooth on the nanoscale, and it is covered with many extended cracks (related to the cooling of the plasma-sprayed titanium).

Surfaces from the second group

The second group gathers all the surfaces designed by subtraction using only blasting and/or etching.

Osseospeed (Figure 4) is produced through blasting with TiO_2 particles and etching with hydrofluoric acid. The surface is impregnated with residual levels of fluoride. No pollution was detected. The microroughness is moderate; it is covered with a nanoroughness all over the implant. Some large TiO_2 residual blasting particles are impacted in the surface and present a very smooth surface. For this reason, the surface may be considered heterogeneous.

Ankylos (Figure 5) is a blasted/etched surface. The surface is covered with alumina particles (Al_2O_3), and many other inorganic pollutions were detected—sodium, fluoride, calcium, phosphorus (as phosphate), zinc, chloride, and sulfur (as sulfate). The surface is moderately microrough and nanosmooth, but it is quite heterogeneous all over the implant.

Zimmer MTX (Figure 6) is produced using blasting with hydroxyapatite on a grade 5 titanium core. Therefore, the surface is impregnated with low levels of calcium phosphate (CaP); it is not visible with FE-SEM but is homogeneous all over the surface. A significant silicon inorganic pollution was also detected. The microroughness is minimal, and the surface is smooth on the nanoscale.

Camlog Promote (Figure 7) is a blasted/etched surface. Some inorganic pollution with zinc and calcium was detected. The surface is moderately microrough and nanosmooth, and it is quite homogeneous all over the implant.

BTI Interna (Figure 8) is an etched surface covered with high levels of organic carbon species (organic pollution). The surface shows numerous aggressive etching pits in a high magnification but with a low height deviation amplitude; thus, the surface has a global smooth aspect on the microscale. At a higher magnification, the topography appears smooth on the nanoscale.

EVL Plus (Figure 9) is a blasted/etched surface. It is impregnated with residual levels

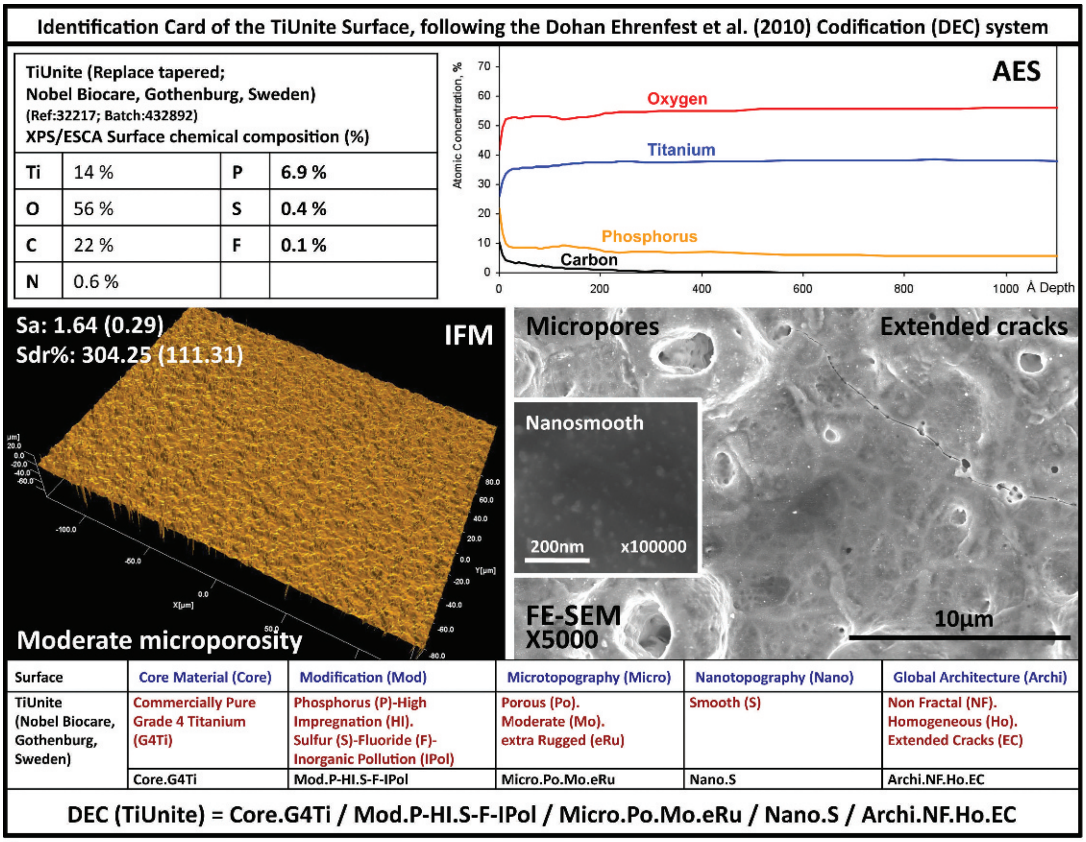

1

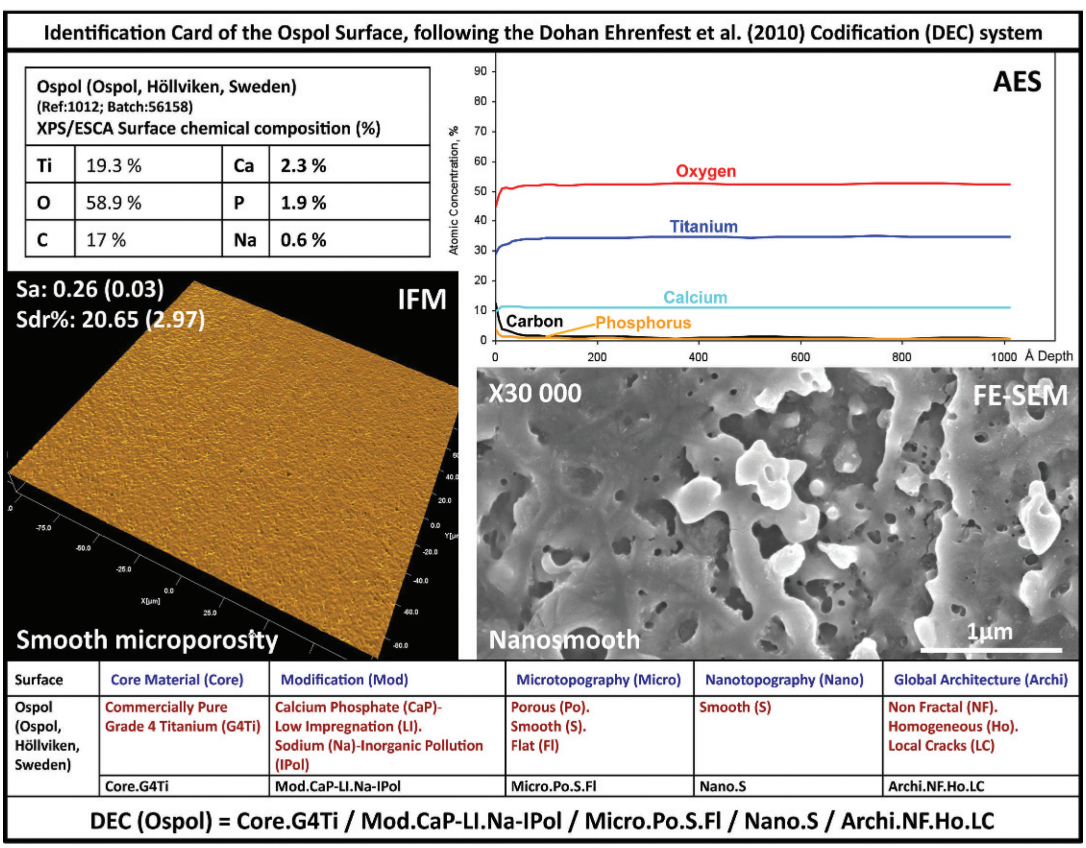

2

Figures 1 and 2. Figure 1. Identification card of the TiUnite surface. **Figure 2.** Identification card of the Ospol surface.

Identification Card of the Kohno HRPS Surface, following the Dohan Ehrenfest et al. (2010) Codification (DEC) system

Kohno HRPS (Sweden & Martina, Due Carrare, Italy)
(Ref:KON-TPS-425-10; Batch:609645.014)
XPS/ESCA Surface chemical composition (%)

Ti	22.8 %	P	0.8 %
O	61.8 %	F	0.7 %
C	11.2 %	S	0.2 %
N	2.5 %		

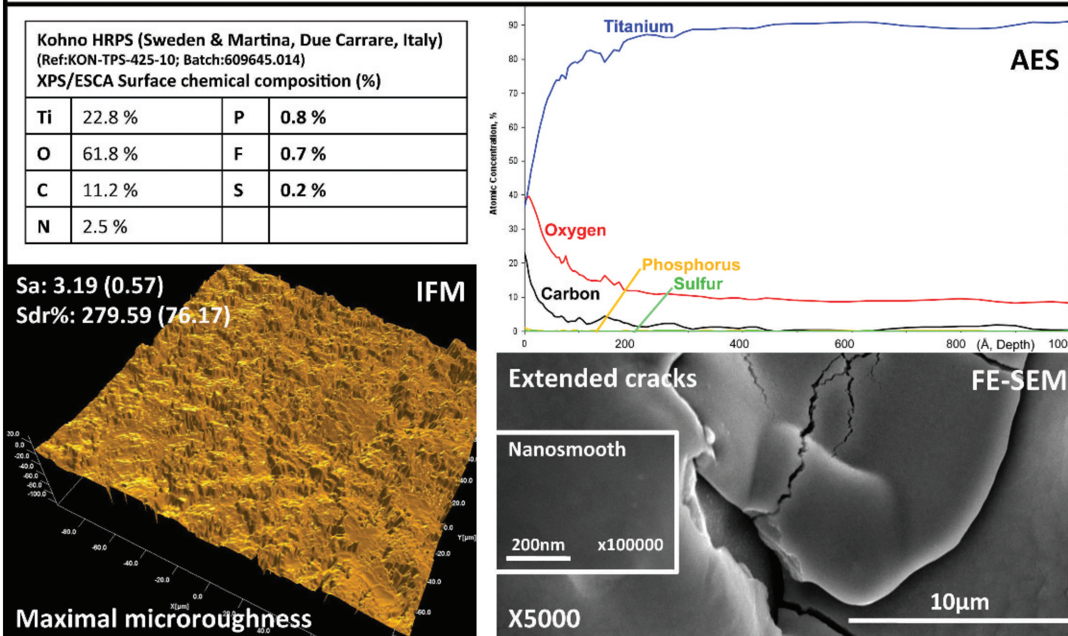

Surface	Core Material (Core)	Modification (Mod)	Microtopography (Micro)	Nanotopography (Nano)	Global Architecture (Archi)
Kohno HRPS (Sweden & Martina, Due Carrare, Italy)	Commercially Pure Grade 2 Titanium (G2Ti)	Phosphorus (P)-Fluoride (F)-Sulfur (S)-Inorganic Pollution (IPol)	Rough (R). Maximal (Ma). extra Rugged (eRu)	Smooth (S)	Non Fractal (NF). Heterogeneous (He). Extended Cracks (EC)
	Core.G2Ti	Mod.P-F-S-IPol	Micro.R.Ma.eRu	Nano.S	Archi.NF.He.EC

DEC (Kohno HRPS) = Core.G2Ti / Mod.P-F-S-IPol / Micro.R.Ma.eRu / Nano.S / Archi.NF.He.EC

3

Identification Card of the Osseospeed Surface, following the Dohan Ehrenfest et al. (2010) Codification (DEC) system

Osseospeed 5.0 S (AstraTech, Mölndal, Sweden)
(Ref:24654; Batch: 60086)
XPS/ESCA Surface chemical composition (%)

Ti	23.9 %
O	60.3 %
C	15.1 %
F	0.7 %

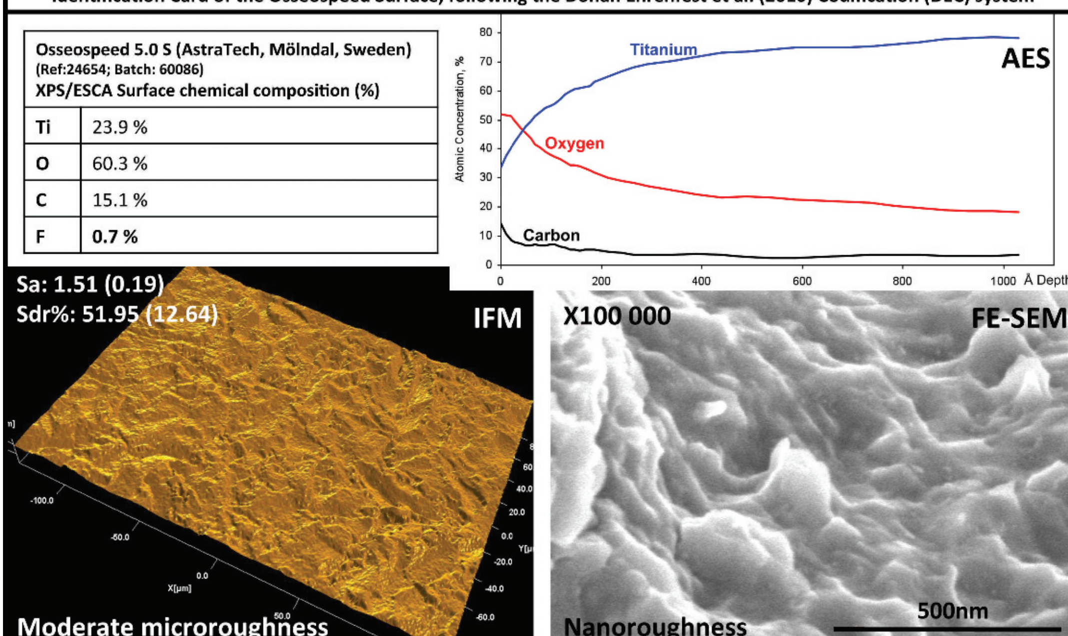

Surface	Core Material (Core)	Modification (Mod)	Microtopography (Micro)	Nanotopography (Nano)	Global Architecture (Archi)
Osseospeed (AstraTech, Mölndal, Sweden)	Commercially Pure Grade 4 Titanium (G4Ti)	Fluoride (F)-Residual Impregnation (RI)	Rough (R). Moderate (Mo). Flattened out (Fo)	Rough (R)	Non Fractal (NF). Heterogeneous (He). TiO_2-Random Particle (TiO_2-RP)
	Core.G4Ti	Mod.F-RI	Micro.R.Mo.Fo	Nano.R	Archi.NF.He.TiO_2-RP

DEC (Osseospeed) = Core.G4Ti / Mod.F-RI / Micro.R.Mo.Fo / Nano.R / Archi.NF.He.TiO_2-RP

4

Figures 3 and 4. Figure 3. Identification card of the Kohno HRPS surface. **Figure 4.** Identification card of the Osseospeed surface.

Identification Card of the Ankylos Surface, following the Dohan Ehrenfest et al. (2010) Codification (DEC) system

Ankylos (Dentsply Friadent, Mannheim, Germany)
(Ref: 31010058; Batch:20015872)
XPS/ESCA Surface chemical composition (%)

Ti	11.1 %	Al	9.8 %	P	0.5 %
O	49.7 %	Na	2.4 %	Zn	0.3 %
C	24.7 %	F	0.7 %	Cl	0.1 %
		Ca	0.6 %	S	<0.1 %

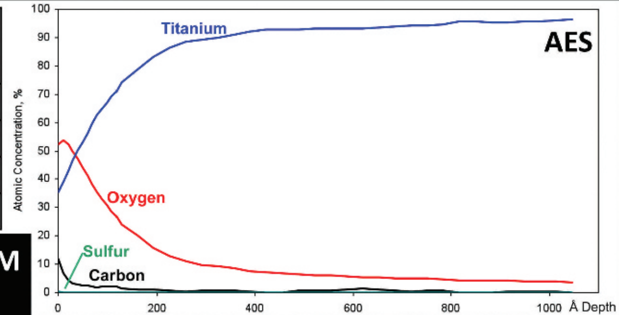

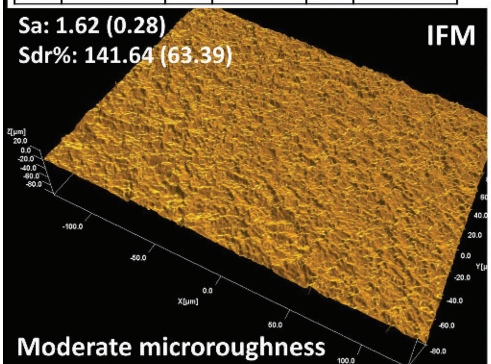

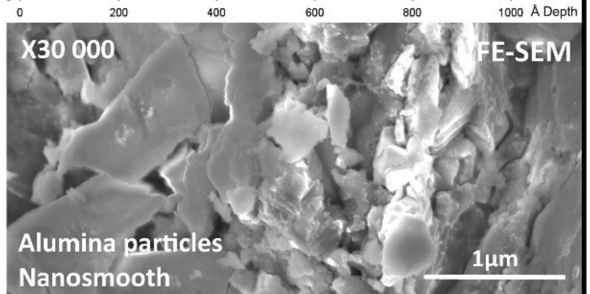

Surface	Core Material (Core)	Modification (Mod)	Microtopography (Micro)	Nanotopography (Nano)	Global Architecture (Archi)
Ankylos (Dentsply Friadent, Mannheim, Germany)	Commercially Pure Grade 2 Titanium (G2Ti)	Aluminium oxide (Al_2O_3)-Sprinkled Coating (SC). Sodium (Na)-Fluoride (F)-Calcium (Ca)-Phosphorus (P)-Zinc (Zn)-Chloride (Cl)-Sulfur (S)-Inorganic Pollution (IPol)	Rough (R). Moderate (Mo). Rugged (Ru)	Smooth (S)	Non Fractal (NF). Heterogeneous (He)
	Core.G2Ti	Mod.Al_2O_3-SC.Na-F-Ca-P-Zn-Cl-S-IPol	Micro.R.Mo.Ru	Nano.S	Archi.NF.He

DEC (Ankylos) = Core.G2Ti / Mod.Al_2O_3-SC.Na-F-Ca-P-Zn-Cl-S-IPol / Micro.R.Mo.Ru / Nano.S / Archi.NF.He

5

Identification Card of the Zimmer MTX Surface, following the Dohan Ehrenfest et al. (2010) Codification (DEC) system

MTX (Tapered Screw-Vent; Zimmer, Carlsbad, CA, USA)
(Ref: TSVB16; Batch:60714527)
XPS/ESCA Surface chemical composition (%)

Ti	15 %	Al	1.4 %
O	54.5 %	Si	3.8 %
C	22.9 %	Ca	0.4 %
N	0.5 %	P	1.5 %

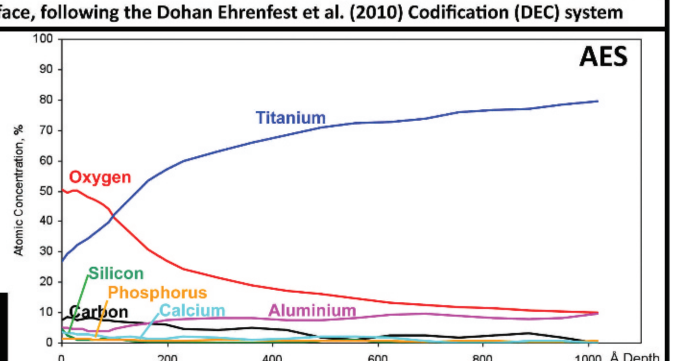

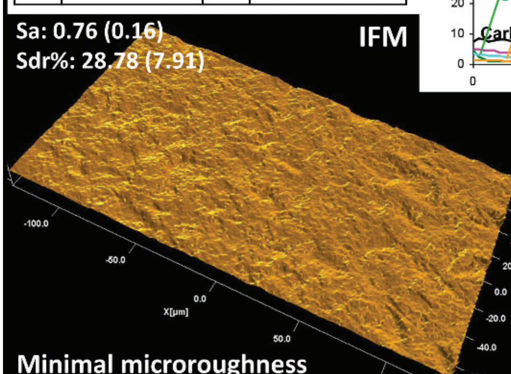

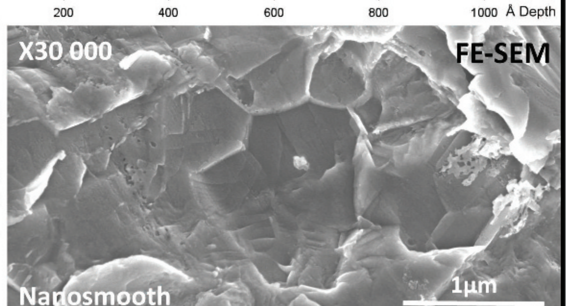

Surface	Core Material (Core)	Modification (Mod)	Microtopography (Micro)	Nanotopography (Nano)	Global Architecture (Archi)
MTX (Zimmer, Carlsbad, CA, USA)	Ti-6Al-4V Grade 5 Titanium (G5Ti)	Calcium Phosphate (CaP)-Low Impregnation (LI). Silicon (Si)-Inorganic Pollution (IPol)	Rough (R). Minimal (Mi). Flat (Fl)	Smooth (S)	Non Fractal (NF). Homogeneous (Ho)
	Core.G5Ti	Mod.CaP-LI.Si-IPol	Micro.R.Mi.Fl	Nano.S	Archi.NF.Ho

DEC (Zimmer MTX) = Core.G5Ti / Mod.CaP-LI.Si-IPol / Micro.R.Mi.Fl / Nano.S / Archi.NF.Ho

6

FIGURES 5 AND 6. FIGURE 5. Identification card of the Ankylos surface. **FIGURE 6.** Identification card of the Zimmer MTX surface.

Identification Card of the Camlog Promote Surface, following the Dohan Ehrenfest et al. (2010) Codification (DEC) system

Promote (Screwline; Camlog, Basel, Switzerland)
(Ref: K1052.5013; Batch:18555)
XPS/ESCA Surface chemical composition (%)

Ti	21.7 %	N	0.5 %
O	51.4 %	Zn	0.3 %
C	25.9 %	Ca	0.2 %

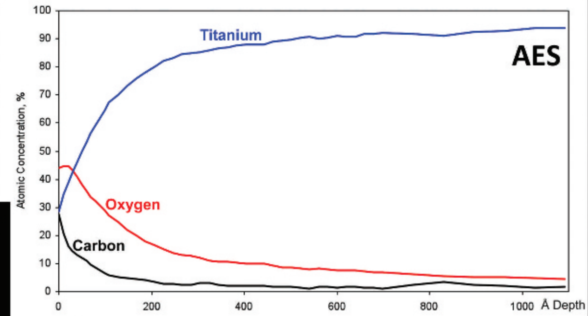

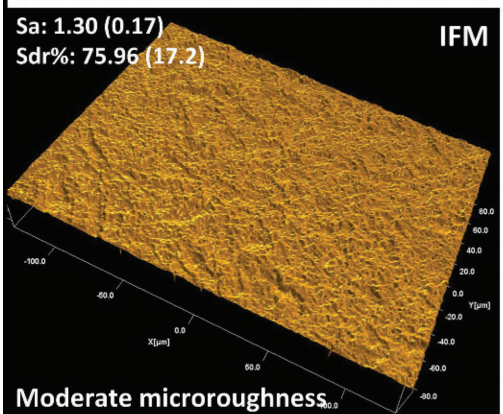

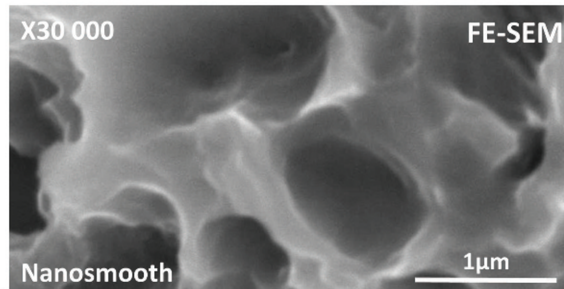

Surface	Core Material (Core)	Modification (Mod)	Microtopography (Micro)	Nanotopography (Nano)	Global Architecture (Archi)
Promote (Camlog, Basel, Switzerland)	Commercially Pure Grade 4 Titanium (G4Ti)	Zinc (Zn)-Calcium (Ca)-Inorganic Pollution (IPol)	Rough (R). Moderate (Mo). Flattened out (Fo)	Smooth (S)	Non Fractal (NF). Homogeneous (Ho)
	Core.G4Ti	Mod.Zn-Ca-IPol	Micro.R.Mo.Fo	Nano.S	Archi.NF.Ho

DEC (Camlog Promote) = Core.G4Ti / Mod.Zn-Ca-IPol / Micro.R.Mo.Fo / Nano.S / Archi.NF.Ho

7

Identification Card of the BTI Interna Surface, following the Dohan Ehrenfest et al. (2010) Codification (DEC) system

BTI Interna (BTI, Vitoria, Spain)
(Ref:IIPS5085; Batch: 2007006999)
XPS/ESCA Surface chemical composition (%)

Ti	16.3 %	N	3 %
O	43 %	Cl	<0.1 %
C	37.6 %		

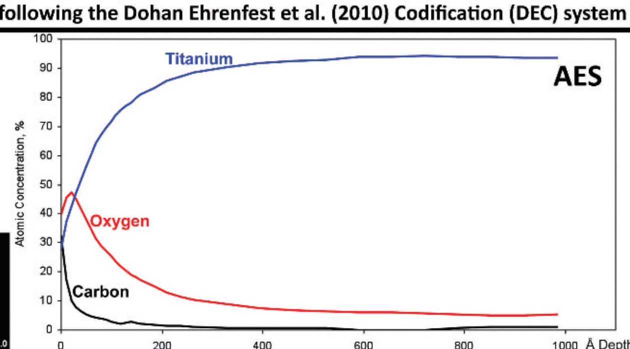

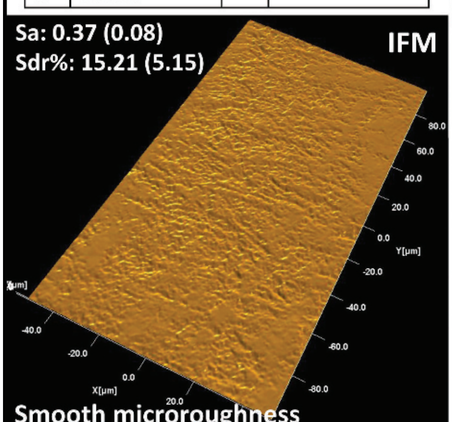

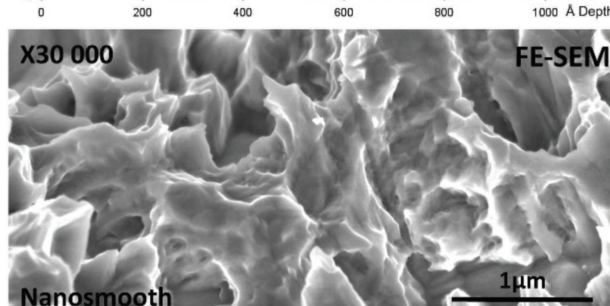

Surface	Core Material (Core)	Modification (Mod)	Microtopography (Micro)	Nanotopography (Nano)	Global Architecture (Archi)
BTI Interna (BTI, Vitoria, Spain)	Commercially Pure Grade 4 Titanium (G4Ti)	Organic Pollution (OPol). Chloride (Cl)-Inorganic Pollution (IPol)	Rough (R). Smooth (S). Flat (Fl)	Smooth (S)	Non Fractal (NF). Homogeneous (Ho)
	Core.G4Ti	Mod.OPol.Cl-IPol	Micro.R.S.Fl	Nano.S	Archi.NF.Ho

DEC (BTI Interna) = Core.G4Ti / Mod.OPol.Cl-IPol / Micro.R.S.Fl / Nano.S / Archi.NF.Ho

8

FIGURES 7 AND 8. FIGURE 7. Identification card of the Camlog Promote surface. **FIGURE 8.** Identification card of the BTI Interna surface.

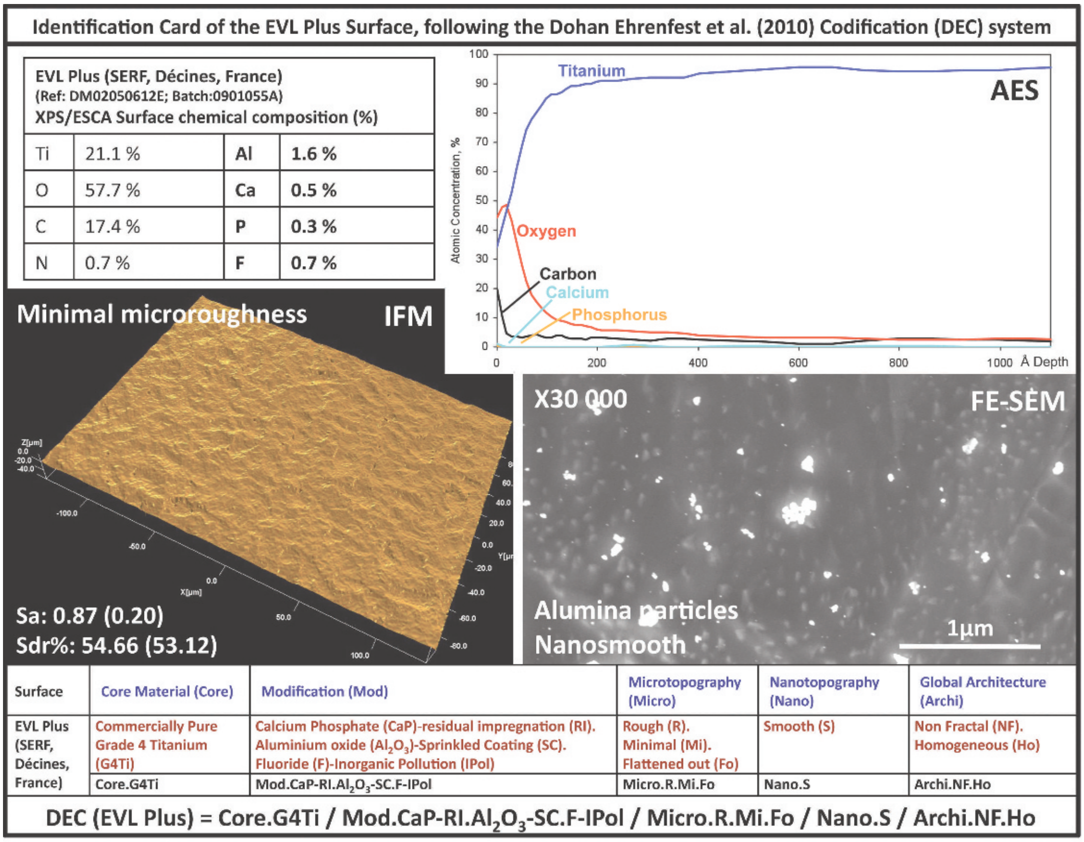

9

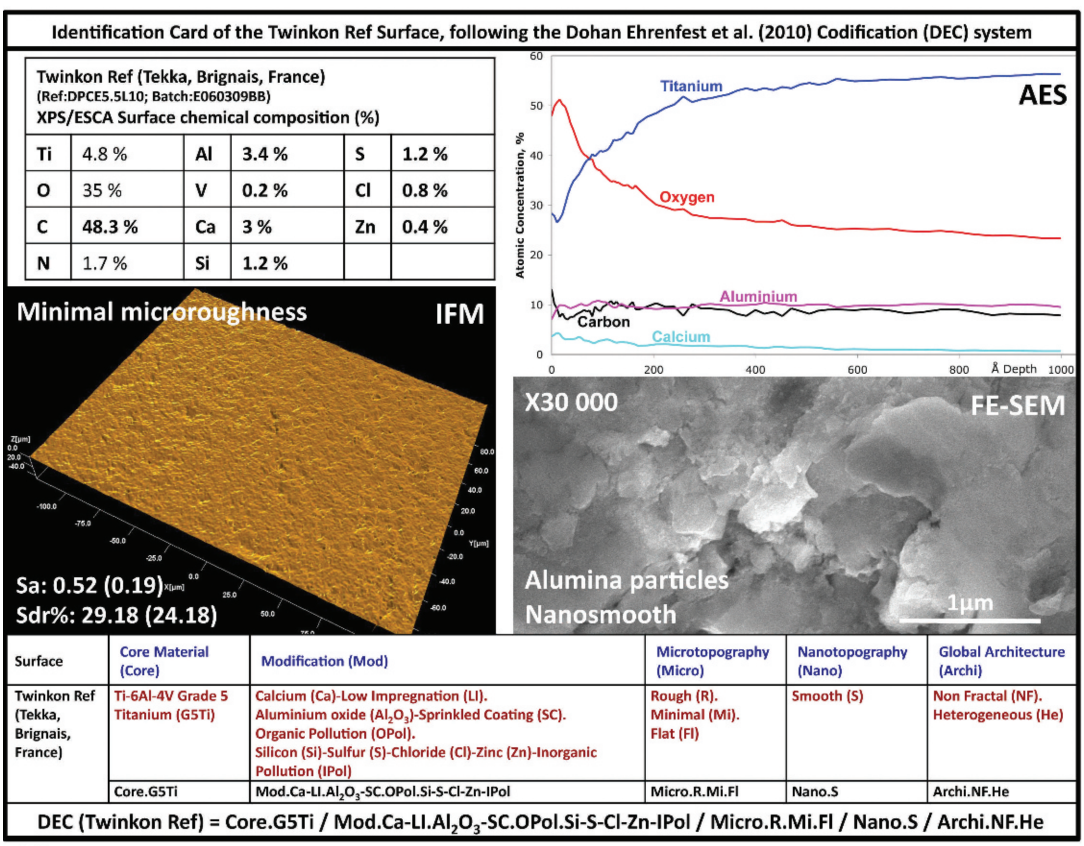

10

Figures 9 and 10. Figure 9. Identification card of the EVL Plus surface. **Figure 10.** Identification card of the Twinkon Ref surface.

of calcium phosphate and covered with small alumina (Al_2O_3) particles. A residual fluoride inorganic pollution was also detected. The microroughness is minimal, and the surface is smooth on the nanoscale.

Twinkon Ref (Figure 10) is a blasted surface on a grade 5 titanium core. The surface appears impregnated with calcium, and it is covered with alumina particles (Al_2O_3) and a thick organic pollution (thick carbon overcoat all over the implant). Some other inorganic pollutions were detected: silicon, sulfur (as sulfate), chloride, and zinc. The surface is minimally microrough, is nanosmooth, and is heterogeneous all over the implant.

Surfaces from the third group

The third group gathers the surfaces designed by subtraction using blasting and/or etching and postprocessing (except coating). In this study, only one product could be classified in this group.

Ossean (Figure 11) is a blasted/etched surface with unknown postprocessing. The TiO_2 layer is thicker than 12 nm. The surface is impregnated with low levels of calcium phosphate, which is not visible with FE-SEM but is homogeneous all over the surface. No pollution was detected. The microroughness is minimal, though close to the moderate level, and it is covered with a nanoroughness all over the implant. The surface is homogeneous in chemistry and topography, and it may be considered fractal according to our definition.

Surfaces from the fourth group

The fourth group gathers the surfaces presenting a final chemical coating.

Of these, 3I NanoTite (Figure 12) is an etched surface on a grade 5 titanium core; it has a final discontinuous coating with CaP particles. Some traces of fluoride and sulfur inorganic pollutions were also detected. The microroughness is smooth and flat, and it is covered with nanoparticles that create a significant texture on the nanoscale. The size of the CaP particles can vary a lot, however, and many microparticles or CaP aggregates are randomly found on the surface. For this reason, the surface should be considered heterogeneous.

SLActive (Figure 13) is a blasted/etched surface with a final immersion in a sodium chloride (NaCl) physiological solution. The surface is therefore coated with NaCl crystals, and some traces of other elements were also detected (fluoride, potassium, calcium, and phosphate). The microtopography is moderately rough and rugged. When the implant is outside its box, the solution dries quickly on the surface and creates many NaCl aggregates all over the implant and a significant nanotexturization. However, the morphology of this coating is very heterogeneous.

Integra-CP, previously known as Bicon NanoTite (Figure 14), is a blasted/etched surface with a final coating using calcium phosphate ion-beam assisted deposition. The CaP coating is thicker than 100 nm, and CaP is therefore the core material of this surface. Some traces of fluoride and sulfur pollutions were also detected. The surface is flat on the microscale and smooth on the nanoscale.

Discussion

Since the osseointegration concept was established, the characteristics of the bone/implant interface and ways to improve it have been analyzed in dental implant research. However, the accurate characterization of the surfaces is still a source of misunderstanding and debate.

The use of these classic instruments for chemical analysis (XPS/ESCA and AES) seems to be a simple and logical approach, but most studies about implant surface still neglect the investigation of the surface chemistry.[2] The chemical characterization of

Identification Card of the Ossean Surface, following the Dohan Ehrenfest et al. (2010) Codification (DEC) system

Ossean (Intra-Lock, Boca Raton, Florida, USA)
(Ref:I4711STI; Batch: AI234)
XPS/ESCA Surface chemical composition (%)

Ti	19.8 %	N	1.5 %
O	57.0 %	P	2.9 %
C	18.5 %	Ca	0.3 %

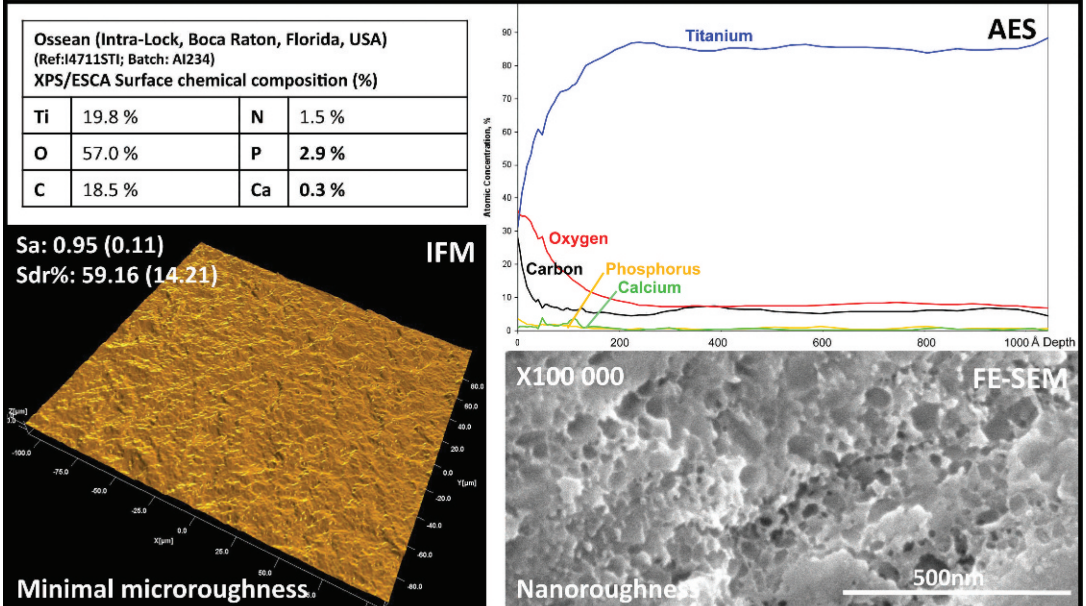

Surface	Core Material (Core)	Modification (Mod)	Microtopography (Micro)	Nanotopography (Nano)	Global Architecture (Archi)
Ossean (Intra-Lock, Boca Raton, Florida, USA)	Commercially Pure Grade 4 Titanium (G4Ti)	Calcium Phosphate (CaP)-Low Impregnation (LI)	Rough (R). Minimal (Mi). Flattened out (Fo)	Rough (R)	Fractal (F). Homogeneous (Ho)
	Core.G4Ti	Mod.CaP-LI	Micro.R.Mi.Fo	Nano.R	Archi.F.Ho

DEC (Ossean) = Core.G4Ti / Mod.CaP-LI / Micro.R.Mi.Fo / Nano.R / Archi.F.Ho

11

Identification Card of the 3I NanoTite Surface, following the Dohan Ehrenfest et al. (2010) Codification (DEC) system

3I NanoTite (Certain Prevail;
Biomet 3I, Palm Beach Gardens, FL, USA)
(Ref:NIIOS4515; Batch:833750)
XPS/ESCA Surface chemical composition (%)

Ti	6 %	Al	0.4 %	F	0.5 %
O	53.9 %	Ca	12.3 %	S	0.3 %
C	18.7 %	P	7.9 %		

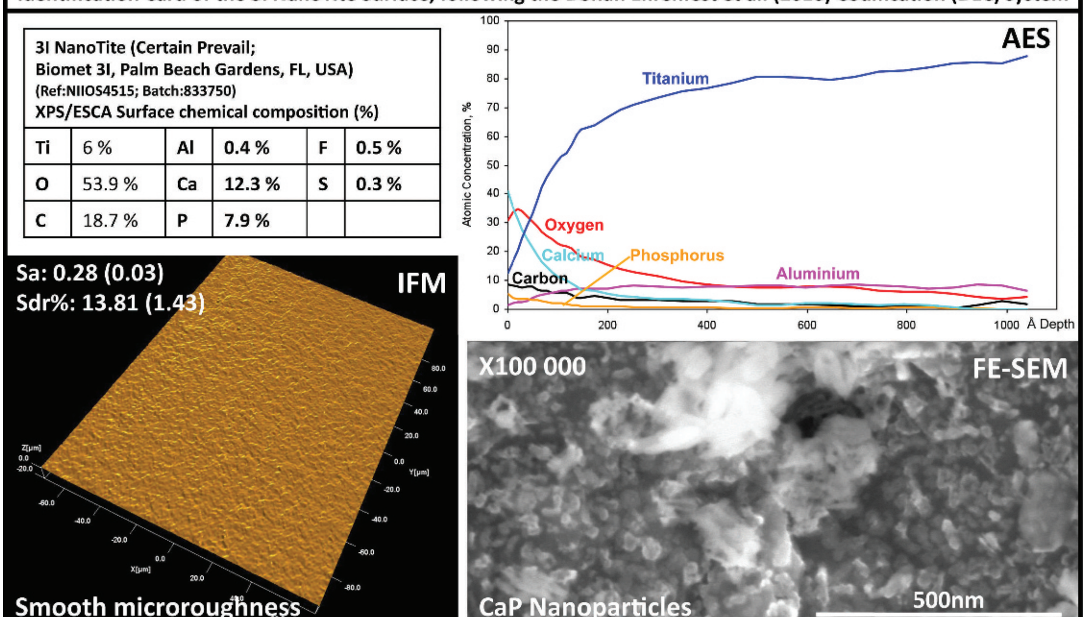

Surface	Core Material (Core)	Modification (Mod)	Microtopography (Micro)	Nanotopography (Nano)	Global Architecture (Archi)
3I NanoTite (Biomet 3I, Palm Beach Gardens, FL, USA)	Ti-6Al-4V Grade 5 Titanium (G5Ti)	Calcium Phosphate (CaP)-Discontinuous Coating (DC). Fluoride (F)-Sulfur (S)-Inorganic Pollution (IPol)	Rough (R). Smooth (S). Flat (Fl)	Calcium Phosphate (CaP)-Particle (Pt)	Non Fractal (NF). Heterogeneous (He)
	Core.G5Ti	Mod.CaP-DC.F-S-IPol	Micro.R.S.Fl	Nano.CaP-Pt	Archi.NF.He

DEC (3I NanoTite) = Core.G5Ti / Mod.CaP-DC.F-S-IPol / Micro.R.S.Fl / Nano.CaP-Pt / Archi.NF.He

12

FIGURES 11 AND 12. FIGURE 11. Identification card of the Ossean surface. **FIGURE 12.** Identification card of the 3I NanoTite surface.

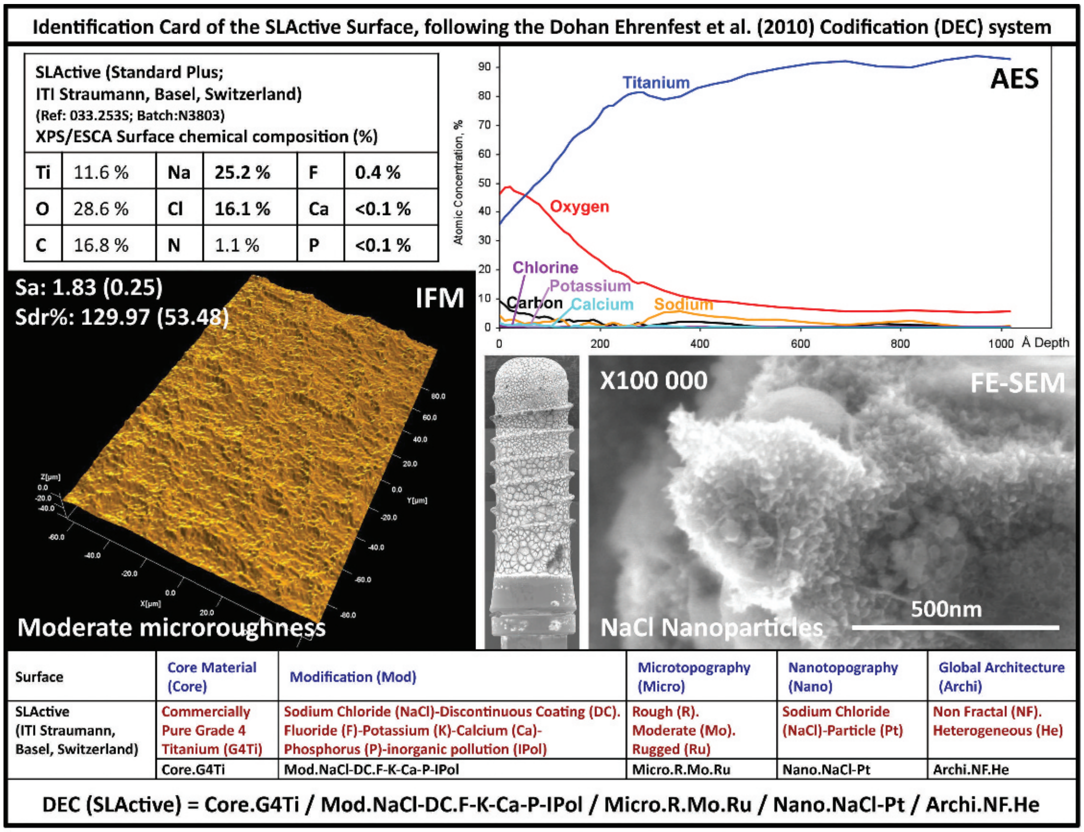

Ti	11.6 %	Na	25.2 %	F	0.4 %
O	28.6 %	Cl	16.1 %	Ca	<0.1 %
C	16.8 %	N	1.1 %	P	<0.1 %

Surface	Core Material (Core)	Modification (Mod)	Microtopography (Micro)	Nanotopography (Nano)	Global Architecture (Archi)
SLActive (ITI Straumann, Basel, Switzerland)	Commercially Pure Grade 4 Titanium (G4Ti)	Sodium Chloride (NaCl)-Discontinuous Coating (DC). Fluoride (F)-Potassium (K)-Calcium (Ca)-Phosphorus (P)-inorganic pollution (IPol)	Rough (R). Moderate (Mo). Rugged (Ru)	Sodium Chloride (NaCl)-Particle (Pt)	Non Fractal (NF). Heterogeneous (He)
	Core.G4Ti	Mod.NaCl-DC.F-K-Ca-P-IPol	Micro.R.Mo.Ru	Nano.NaCl-Pt	Archi.NF.He

DEC (SLActive) = Core.G4Ti / Mod.NaCl-DC.F-K-Ca-P-IPol / Micro.R.Mo.Ru / Nano.NaCl-Pt / Archi.NF.He

13

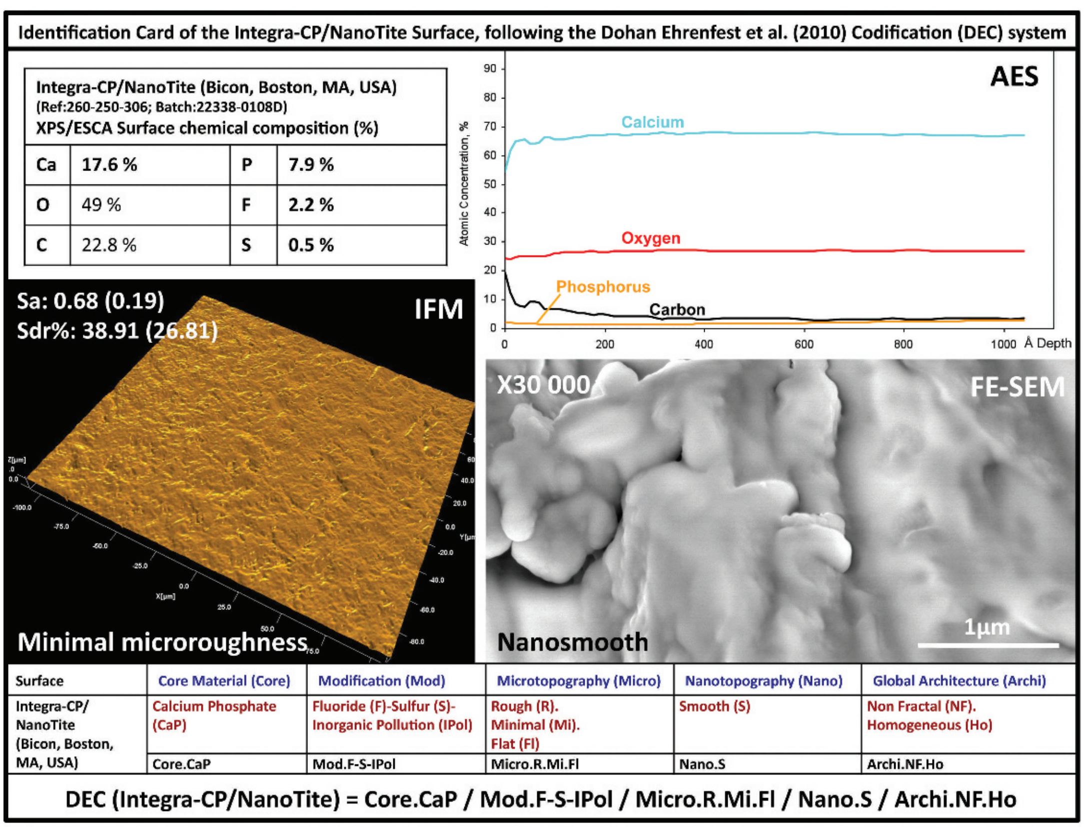

Ca	17.6 %	P	7.9 %
O	49 %	F	2.2 %
C	22.8 %	S	0.5 %

Surface	Core Material (Core)	Modification (Mod)	Microtopography (Micro)	Nanotopography (Nano)	Global Architecture (Archi)
Integra-CP/NanoTite (Bicon, Boston, MA, USA)	Calcium Phosphate (CaP)	Fluoride (F)-Sulfur (S)-Inorganic Pollution (IPol)	Rough (R). Minimal (Mi). Flat (Fl)	Smooth (S)	Non Fractal (NF). Homogeneous (Ho)
	Core.CaP	Mod.F-S-IPol	Micro.R.Mi.Fl	Nano.S	Archi.NF.Ho

DEC (Integra-CP/NanoTite) = Core.CaP / Mod.F-S-IPol / Micro.R.Mi.Fl / Nano.S / Archi.NF.Ho

14

Figures 13 and 14. Figure 13. Identification card of the SLActive surface. **Figure 14.** Identification card of the Integra-CP/NanoTite surface.

commercially available products is also quite scarce in the literature.[34,35] In contrast, the evaluation of the surface morphology and topography on the micrometer scale is commonly used, but the way to quantify the microstructures remains a source of debate, particularly because data are very dependent on the instrument and protocol used.[36] Finally, the investigation of the nanotopography of dental implants is a very recent approach.[37–39]

The concept of these ID cards is to gather the main information concerning a surface in a simple and standardized way. However, it is very important to understand the limitations of such a system. The chemical analyses are accurate but are always difficult to interpret completely without detailed spectrometric graphs and the knowledge of how to read them.[35] The IFM mean values of the microtopography also have to be considered as relative, because such values are always dependent on the method used (measuring equipment, filtering technique, number and size of measure areas).[36] Finally, the notions of nanosmooth/nanorough are only qualitative and morphological and, like most other terms used in the codification system, are based on the definitions given in the classification article.[2] Other authors may prefer to use different terms or interpretations.[38] This is why the codes are called "DEC": the data here are sorted and interpreted following a specific and well-defined system, and some differences can appear in the terminology used by other authors. Therefore, the ID cards and the DEC system must be considered as a tool, not as absolute data. When considering all of these codes obtained by the same protocol, it is possible to compare the main characteristics of the various implant surfaces together.

The notion of surface homogeneity is also to be understood with caution. Even if dental implants are supposed to be carefully manufactured products, most implants are not as homogeneous as expected, though this is considered as normal. Therefore, in the codification system, the homogeneity of a surface should be understood as a relative homogeneity, that is, implants are all homogeneous unless they are clearly heterogeneous. The reasons for this heterogeneity are numerous but always quite simple to understand: when some areas of the surface are lacking a key characteristic of the other areas (eg, Osseospeed smooth TiO_2 blasting residues), when the crystal clusters cannot be controlled (eg, SLActive, NanoTite), or when the surfaces are covered by various kinds of pollutions (eg, Ankylos, Tekka). In this classification system, it remains a qualitative parameter, not a quantitative one.

The first objective of the DEC[2] system was to create a standard procedure for the characterization of surfaces in order to define and isolate more clearly the chemical and physical parameters when comparing the biological performances of various surfaces. It was therefore first an experimental tool.

The second objective of the DEC system is directly related to the development of the surface ID card: to create a standard procedure for describing and controlling commercially available products. Nowadays, there is no serious standard that defines what a surface should be, and dental implants are marketed without a clear definition of their surface characteristics. This lack of surface characterization is common to many implantable biomedical devices. Therefore, the practitioner has no real information about the material that is implanted in his or her patients, though the practitioner is partially responsible for these implanted materials. This situation is contradictory, and may be legally dangerous, when considering that the surface design defines the interface of the biomaterial with the host tissues and thus represents a key component of the implant biocompatibility.

The use of the DEC system on a product ID card that gathers the main surface data is a simple way to provide this key information to practitioners. However, these analyses and the establishment of these ID cards should always be performed by independent teams without conflict of interest and should be repeated frequently within the various references and batches of the company's production to guarantee the validity of the codes. The DEC system could, therefore, be a first step toward the development of an ISO characterization standard procedure in order to increase the control of the available products. This is of particular interest because the globalization of implant production means many implants are produced in unknown conditions in various countries with different regulations and are marketed without any serious control. The establishment and regular control of a DEC system by a renowned team could therefore offer a supplementary guarantee to the users.

We also noticed that some surfaces were very heterogeneous, and therefore may present different codes (chemical and/or morphological) depending on the area of analysis. Theoretically, the surface is a very significant characteristic of the product, and Food and Drug Administration approvals (or other administrative agreements) are given for one specific product. The industrial production under an administrative approval is supposed to be homogeneous. When companies are producing implants with different surfaces depending on the batch, logically these batches have to be considered as different products. This situation raises serious legal issues, and some companies should check their productions more carefully and identify their surfaces in order to avoid misunderstandings and potential serious legal consequences.

Finally, during the establishment of these ID cards, we noticed that some surfaces were not clearly named (and trademarked) by the companies, as if the surfaces were not a specific characteristic of the products. For clarity reasons, all surfaces should be clearly named. If different versions of the surface exist, different name variations (for example with a 1.0, 2.0, 2.1, marking) should be used. A well-characterized surface, with a specific name that refers to a specific product, would be the ideal situation from an industrial and legal/administrative standpoint.

Conclusions

The development of the DEC system is a way to establish a standard for the characterization of implant surfaces. The purpose of this systematic and simple approach is first to clarify the experimental data published in the literature in order to make it easier to sort and interpret. The presentation of the DEC system on an ID card is also of great practical interest for the implant users, as it allows the main characteristics of commercially available surfaces to be gathered in a reader-friendly document. This ID card gives the necessary information to the surgeon when selecting an implant system for daily practice. This is of particular interest as practitioners are legally responsible for the choice of their implantable materials. Finally, the use of the DEC system could be an interesting basis for the development of a clear and simple ISO standard for dental implant surfaces and for other implants, such as orthopedic implantable devices.

Abbreviations

AES: Auger electron spectroscopy

DEC: Dohan Ehrenfest et al (2010) Codification

ESCA: electron spectroscopy for chemical analysis

FE-SEM: field emission-scanning electron microscope

IFM: interferometer

SEM: scanning electron microscope
TPS: titanium plasma-sprayed
XPS: x-ray photoelectron spectroscopy

Acknowledgments

This work was partially supported by a grant from the LoB5 Foundation for Research, Paris, France. The authors want to thank particularly Thomas Fister, Brad Burrow, Lori Bisaha, Shannon Xia, Philippe Leclercq, Philippe Russe, and Marco Del Corso for their technical help in this work.

Note

This codification article does not give qualitative opinions and is strictly founded on physical and chemical definitions to avoid any subconscious conflict of interest. Moreover, the chemical values (XPS/AES) and the morphological data shown in the ID cards were obtained by an independent laboratory and were always double-checked by the team. This work was not supported by grants from any commercial companies.

References

1. Winkler S, Morris HF. Dental implant research: a perspective. *J Oral Implantol*. 2009;35:3–4.
2. Dohan Ehrenfest DM, Coelho PG, Kang BS, Sul YT, Albrektsson T. Classification of osseointegrated implant surfaces: materials, chemistry and topography. *Trends Biotechnol*. 2010;28:198–206.
3. Ahn SJ, Leesungbok R, Lee SW. Histomorphometric analysis and removal torque of small diameter implants with alternative surface treatments and different designs. *J Oral Implantol*. 2010;36:263–272.
4. Flanagan D. Calcium hydroxide paste as a surface detoxifying agent for infected dental implants: two case reports. *J Oral Implantol*. 2009;35:204–209.
5. Franco M, Rigo L, Viscione A, et al. CaPO(4) blasted implants inserted into iliac crest homologue frozen grafts. *J Oral Implantol*. 2009;35:176–180.
6. Mangano C, Piattelli A, d'Avila S, et al. Early human bone response to laser metal sintering surface topography: a histologic report. *J Oral Implantol*. 2010;36:91–96.
7. Sul YT. The significance of the surface properties of oxidized titanium to the bone response: special emphasis on potential biochemical bonding of oxidized titanium implant. *Biomaterials*. 2003;24:3893–3907.
8. Sul YT, Kang BS, Johansson C, Um HS, Park CJ, Albrektsson T. The roles of surface chemistry and topography in the strength and rate of osseointegration of titanium implants in bone. *J Biomed Mater Res A*. 2009;89:942–950.
9. Luongo G, Oteri G. A noninterventional study documenting use and success of implants with a new chemically modified titanium surface in daily dental practice. *J Oral Implantol*. 2010;36:305–314.
10. Malchiodi L, Corrocher G, Cucchi A, Ghensi P, Bissolotti G, Nocini PF. Long-term results of immediately loaded fast bone regeneration-coated implants placed in fresh extraction sites in the upper jaw. *J Oral Implantol*. 2010;36:251–262.
11. Carinci F, Brunelli G, Danza M. Platform switching and bone platform switching. *J Oral Implantol*. 2009;35:245–250.
12. Chong L, Khocht A, Suzuki JB, Gaughan J. Effect of implant design on initial stability of tapered implants. *J Oral Implantol*. 2009;35:130–135.
13. Irinakis T, Wiebe C. Initial torque stability of a new bone condensing dental implant. A cohort study of 140 consecutively placed implants. *J Oral Implantol*. 2009;35:277–282.
14. Irinakis T, Wiebe C. Clinical evaluation of the Nobelactive implant system: a case series of 107 consecutively placed implants and a review of the implant features. *J Oral Implantol*. 2009;35:283–288.
15. Park YS, Lee SP, Han CH, Kwon JH, Jung YC. The microtomographic evaluation of marginal bone resorption of immediately loaded scalloped design implant with various microthread configurations in canine mandible: pilot study. *J Oral Implantol*. 2010;36:357–362.
16. Pellizzer EP, Falcon-Antenucci RM, de Carvalho PSP, Santiago JF, de Moraes SLD, de Carvalho BM. Photoelastic analysis of the influence of platform switching on stress distribution in implants. *J Oral Implantol*. 2010;36:419–424.
17. Simonpieri A, Del Corso M, Sammartino G, Dohan Ehrenfest DM. The relevance of Choukroun's platelet-rich fibrin and metronidazole during complex maxillary rehabilitations using bone allograft. Part I: a new grafting protocol. *Implant Dent*. 2009;18:102–111.
18. Simonpieri A, Del Corso M, Sammartino G, Dohan Ehrenfest DM. The relevance of Choukroun's platelet-rich fibrin and metronidazole during complex maxillary rehabilitations using bone allograft. Part II: implant surgery, prosthodontics, and survival. *Implant Dent*. 2009;18:220–229.
19. Flanagan D. Stress related peri-implant bone loss. *J Oral Implantol*. 2010;36:325–327.
20. Berley J, Yamano S, Sukotjo C. The effect of systemic nicotine on osseointegration of titanium implants in the rat femur. *J Oral Implantol*. 2010;36:185–194.
21. d'Avila S, dos Reis LD, Piattelli A, et al. Impact of smoking on human bone apposition at different dental implant surfaces: a histologic study in type IV bone. *J Oral Implantol*. 2010;36:85–90.
22. Quintero DG, Winger JN, Khashaba R, Borke JL. Advanced glycation endproducts and rat dental implant osseointegration. *J Oral Implantol*. 2010;36:97–104.

23. Winkler S. Extraordinary implant failure. *J Oral Implantol*. 2010;36:391–400.
24. Elo JA, Herford AS, Boyne PJ. Implant success in distracted bone versus autogenous bone-grafted sites. *J Oral Implantol*. 2009;35:181–184.
25. Viscioni A, Rigo L, Franco M, et al. Reconstruction of severely atrophic jaws using homografts and simultaneous implant placement: A retrospective study. *J Oral Implantol*. 2010;36:131–140.
26. Cohen O, Gabay E, Machtei EE. Cooling profile following prosthetic preparation of 1-piece dental implants. *J Oral Implantol*. 2010;36:273–280.
27. Padmanabhan TV, Gupta RK. Comparison of crestal bone loss and implant stability among the implants placed with conventional procedure and using osteotome technique: a clinical study. *J Oral Implantol*. 2010;36:475–483.
28. Simonpieri A, Choukroun J, Del Corso M, Sammartino G, Dohan Ehrenfest DM. Simultaneous sinus-lift and implantation using microthreaded implants and leukocyte- and platelet-rich fibrin as sole grafting material: a six-year experience. *Implant Dent*. 2011;20:2–12.
29. Mazor Z, Horowitz RA, Del Corso M, Prasad HS, Rohrer MD, Dohan Ehrenfest DM. Sinus floor augmentation with simultaneous implant placement using Choukroun's platelet-rich fibrin as the sole grafting material: a radiologic and histologic study at 6 months. *J Periodontol*. 2009;80:2056–2064.
30. Birdi H, Schulte J, Kovacs A, Weed M, Chuang SK. Crown-to-implant ratios of short-length implants. *J Oral Implantol*. 2010;36:425–433.
31. Bilhan H, Mumcu E, Arat S. The role of timing of loading on later marginal bone loss around dental implants: a retrospective clinical study. *J Oral Implantol*. 2010;36:363–376.
32. Flanagan D, Ilies H, Lasko B, Stack J. Force and movement of non-osseointegrated implants: an in vitro study. *J Oral Implantol*. 2009;35:270–276.
33. Romanos G, Froum S, Hery C, Cho SC, Tarnow D. Survival rate of immediately vs delayed loaded implants: analysis of the current literature. *J Oral Implantol*. 2010;36:315–324.
34. Morra M, Cassinelli C, Bruzzone G, et al. Surface chemistry effects of topographic modification of titanium dental implant surfaces: 1. Surface analysis. *Int J Oral Maxillofac Implants*. 2003;18:40–45.
35. Kang BS, Sul YT, Oh SJ, Lee HJ, Albrektsson T. XPS, AES and SEM analysis of recent dental implants. *Acta Biomater*. 2009;5:2222–2229.
36. Wennerberg A, Albrektsson T. Suggested guidelines for the topographic evaluation of implant surfaces. *Int J Oral Maxillofac Implants*. 2000;15:331–344.
37. Melin Svanborg L, Andersson M, Wennerberg A. Surface characterization of commercial oral implants on the nanometer level. *J Biomed Mater Res B Appl Biomater*. 2010;92:462–469.
38. Wennerberg A, Albrektsson T. On implant surfaces: a review of current knowledge and opinions. *Int J Oral Maxillofac Implants*. 2010;25:63–74.
39. Bucci-Sabattini V, Cassinelli C, Coelho PG, Minnici A, Trani A, Dohan Ehrenfest DM. Effect of titanium implant surface nanoroughness and calcium phosphate low impregnation on bone cell activity in vitro. *Oral Surg Oral Med Oral Pathol Oral Radiol Endod*. 2010;109:217–224.
40. Albrektsson T, Wennerberg A. Oral implant surfaces: Part 1–review focusing on topographic and chemical properties of different surfaces and in vivo responses to them. *Int J Prosthodont*. 2004;17:536–543.
41. Sul YT, Johansson CB, Roser K, Albrektsson T. Qualitative and quantitative observations of bone tissue reactions to anodised implants. *Biomaterials*. 2002;23:1809–1817.